

# Nonlinear optical and spectral features of the natural dye derived from *chrysanthemum* petals

C. DEEPA<sup>1</sup>, NATARAJAN ARUMUGAM<sup>2</sup>, ABDULRAHMAN I. ALMANSOUR<sup>2</sup>, P. SANGEETHA<sup>3</sup>, G. MURALI<sup>4</sup>, S. JEYARAM<sup>5,\*</sup>

<sup>1</sup>Department of Physics, Sri Sairam Institute of Technology, West Tambaram, Chennai-600044, Tamilnadu, India

<sup>2</sup>Department of Chemistry, College of Science, King Saud University, P.O. Box 2455, Riyadh 11451, Saudi Arabia

<sup>3</sup>Department of Physics, Panimalar Engineering College, Chennai-600123, Tamilnadu, India

<sup>4</sup>Scientific Officer, Nanotechnology Research Centre, SRM Institute of Science and Technology, SRM Nagar, Kattankulathur-603203, Tamilnadu, India

<sup>5</sup>Department of Physics, Takshashila University, Ongur (PO), Tindivanam (TK), Villupuram-604305, Tamilnadu, India

This work reports to the study of third-order nonlinear optical (NLO) susceptibility ( $\chi^3$ ) and second-order hyperpolarizability ( $\gamma$ ) of a natural dye obtained from chrysanthemum petals. The FT-IR method was utilized to identify the functional groups present in the natural dye. The GC-Mass spectrum was used to find the elemental composition of the pigment. The experiment was carried out using a Z-scan apparatus with a continuous-wave (CW) laser operating at 405 nm wavelength. The closed aperture (CA) and open aperture (OA), were used to measure the natural dye's nonlinear index of refraction ( $n_2$ ) and nonlinear coefficient of absorption ( $\beta$ ). The values of  $n_2$  and  $\beta$  showcased distinct self-defocusing and reverse saturable absorption (RSA) characteristics of the natural dye. The refractive index and absorption coefficient of the dye were determined to be  $4.29 \times 10^{-7} \text{ cm}^2/\text{W}$  and  $2.01 \times 10^{-2} \text{ cm/W}$ , respectively. The third-order NLO susceptibility of the dye was measured to be  $1.41 \times 10^{-6} \text{ esu}$ , while its second-order hyperpolarizability was calculated to be  $1.02 \times 10^{-30} \text{ esu}$ . The study concluded that the natural dye extracted from chrysanthemum petals could be utilized as a suitable NLO material with potential applications in photonics and optoelectronics.

(Received October 2, 2024; accepted April 15, 2025)

**Keywords:** NLO, Chrysanthemum petals, Third-order NLO susceptibility, Nonlinear index of refraction, Nonlinear coefficient of absorption, Thermo-optic coefficient

## 1. Introduction

In recent years, there has been significant interest in nonlinear optical (NLO) materials due to their potential applications in optoelectronics and photonics [1–7]. These applications include time-reversed optical waves, photonics-based computation, optical switching, optical communication, 3D photon imaging, and optical limiting [8–12]. Researchers are exploring both organic and inorganic materials for NLO applications, including optical limiting, switching, and communication, because of their exceptional optical properties. While many inorganic materials have desirable NLO characteristics, their practical use is limited due to their high cost. To address these limitations, researchers are constantly searching new materials with easily obtainable NLO properties and significant features that can be activated by low-power laser stimuli. Flavonoids, anthocyanins, chlorophylls, and carotenoids are the natural pigments with unique optical and chemical characteristics [13–14]. These pigments offer an environmentally friendly, alternative to inorganic and synthetic substances, with simplicity, ecological conservation, cost-effectiveness, and lack of toxicity. A recent advanced study has confirmed the presence of NLO properties in animal dyes derived from flower petals, leaves, bark, seeds, and other natural ingredients, suggesting their potential use in various fields [13–16].

Researchers have employed various methods to investigate the optical nonlinearities, including beam distortion [17], nonlinear interferometry [18], degenerate four-wave and three wave mixing [19], third-harmonic generation [20–21], spatial self-phase modulation [22–23], and Z-scan method [24]. The first four methods require advanced experimental equipment. Comprehensive studies on wave propagation are necessary to ensure the accuracy of experiments involving beam distortion. The single-beam Z-scan technique, developed by Sheikh-Bahae et al., is the predominant experimental method for analyzing NLO properties and it is widely regarded as an effective and valuable approach [24]. The distinguishing feature of the Z-scan approach's setup configuration is its ability to simultaneously measure the nonlinear refractive index ( $n_2$ ) and the nonlinear absorption coefficient ( $\beta$ ). This method quantifies the real and imaginary components of the sample's third-order NLO characteristics. Moreover, the values of  $n_2$  and  $\beta$  can be accurately estimated using the transmittance curve [24]. The aim of this study is to investigate the third-order NLO characteristics of a natural dye obtained from chrysanthemum petals. A low-power diode laser with a wavelength of 405 nm is used to study the NLO properties of the natural dye. The natural dye is further characterized by UV-visible absorption, GC-MS, and FT-IR techniques.

## 2. Experimental details

The *chrysanthemum* petals used in this experiment were purchased from a nearby flower market, and a total of 50 g of flower petals were utilized. The petals were submerged in a round-bottom flask containing 100 mL of distilled water. The mixture was agitated using a magnetic stirrer at a temperature of 30 °C for a duration of 1 hour. The solution was then filtered using filter paper to obtain a transparent yellow pigment, which was subsequently stored in the refrigerator for future use.

The Z-scan approach was employed to quantify the third-order NLO characteristics of the natural dye extracted from chrysanthemum petals. A low-power laser with a wavelength of 405 nm and a power output of 5 mW served as the excitation source. The input intensity at the focus was 745 W/cm<sup>2</sup>. A convex lens with a focal length of 5 cm was used to focus the beam, and a 1 mm thick glass cell was used to collect the natural dye. The glass cell was positioned on a micrometer stage that could be adjusted in the direction of propagation. To measure the sample's transmittance in both the closed-aperture (CA) and open-aperture (OA) modes, a power meter was placed in the far-field region. The thin sample condition was validated owing to the measured Rayleigh length was greater than sample length. Fig. 1 provides a schematic representation of the Z-scan approach.

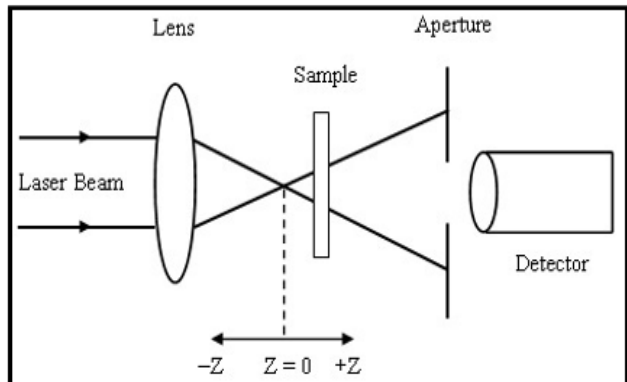


Fig. 1. Z-scan experimental setup

## 3. Results and discussion

### 3.1. UV-Visible absorption study of the natural dye

The UV-visible absorption spectrum of the natural dye obtained from chrysanthemum petals is shown in Fig. 2.

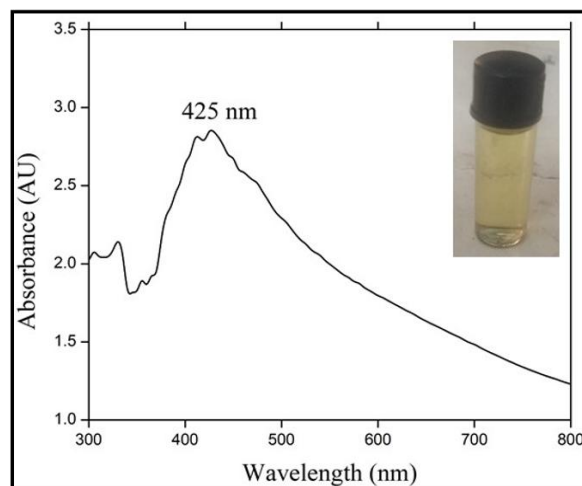


Fig. 2. UV-Visible spectrum of the natural dye derived from chrysanthemum petals (color online)

The curve in the graph represents the portion of the visible region. We observed the highest absorption level at a wavelength of 425 nm, which is due to a low-energy  $\pi$ - $\pi^*$  transition [25]. The natural dye's linear absorption coefficient is determined by.

$$\alpha = 2.303 \times \frac{A}{d} \quad (1)$$

In the equation, A represents the absorbance of the natural dye, while d represents the thickness of the sample.

### 3.2. FT-IR result of the natural dye

Fig. 3 shows the FT-IR image of the natural dye derived from chrysanthemum petals. The frequency allocations are denoted using a standardised infrared (IR) table. A frequency at 1029 cm<sup>-1</sup> was strongly suggests the presence of an asymmetric C-O-C group. The presence of a prominent peak at 1632 cm<sup>-1</sup> indicates that the C=C stretching group. The stretching of the C=C bond is responsible for the molecule exhibiting substantial NLO capabilities. The frequency band at 1881 cm<sup>-1</sup> corresponds to the C-H bending of the alkene group, whereas the frequency band at 2103 cm<sup>-1</sup> corresponds to the stretching of the alkene group.

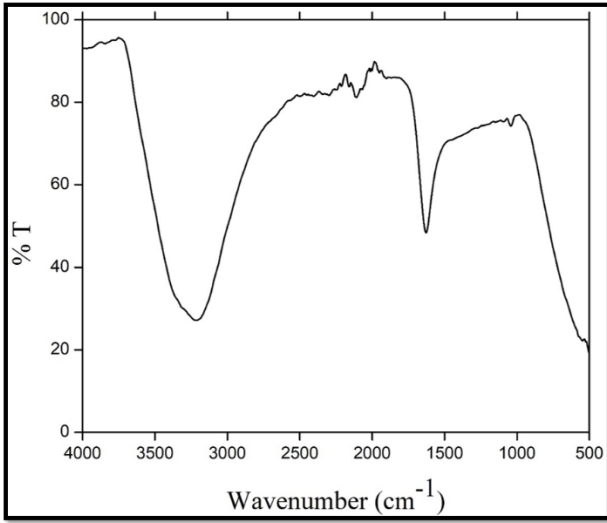


Fig. 3. FT-IR spectrum of the natural dye derived from *chrysanthemum* petals

### 3.3. GC-Mass spectrum of the natural dye

The gas chromatography mass spectrum of natural dye extracted from *chrysanthemum* petals is shown in Fig. 4. From Fig. 4, the available oil components including  $\alpha$ -Pinene (9.099), Artemisia alcohol (12.513), Terpinen-4-ol (15.348), Hexyl isovalerate (16.544), Eugenol (19.228),  $\alpha$ -Guaiane (21.014) and  $\beta$ -Bisabolene (22.663) were present.

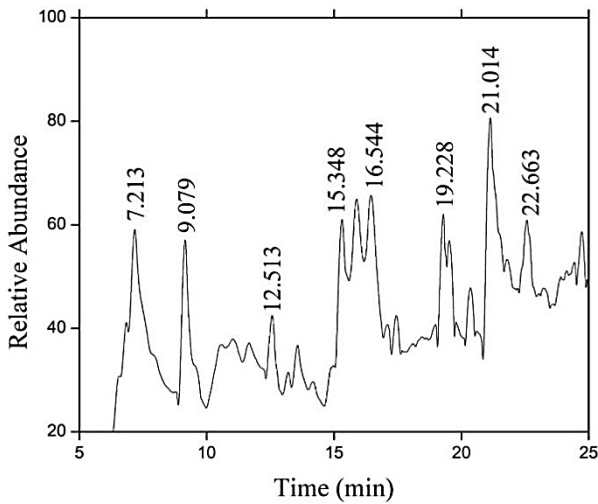


Fig. 4. GC-MS of natural dye derived from *chrysanthemum* petals

### 3.4. Third-order NLO characteristics of the natural dye

The OA and CA Z-scan apparatuses were used to find the third-order NLO properties of the natural dye obtained from *chrysanthemum* petals [24]. The OA method is used to calculate the  $\beta$  of the natural dye, which has a direct relationship with the imaginary features of the third-order

NLO susceptibility. The dye's  $n_2$  value is determined by the CA configuration which is directly related to the real component of the third-order nonlinear optical susceptibility. It is possible to figure out the third-order NLO susceptibility of the natural dye obtained from *chrysanthemum* petals by adding up the real and imaginary parts of the third-order NLO susceptibility [24]. Fig. 5 displays the OA profile of the natural dye obtained from *chrysanthemum* petals. The natural dye exhibits reverse saturable absorption (RSA), and a significant interaction takes place at the focal point between the natural dye and the light beam.

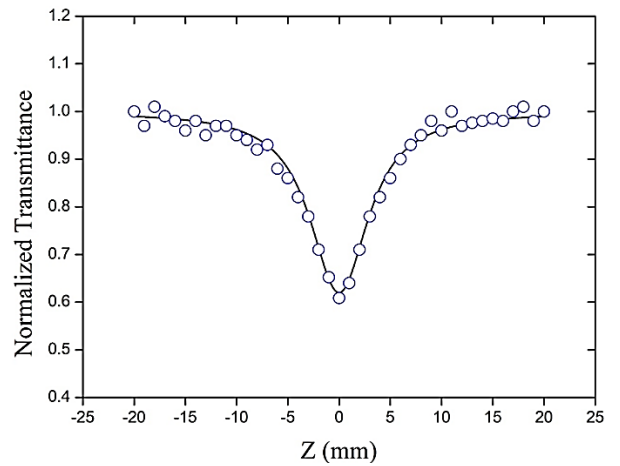


Fig. 5. OA Z-scan result of the natural dye derived from *chrysanthemum* petals (color online)

Consequently, the absorption of photons significantly rises at the focal point, leading to a noticeable decrease in transmittance at that location. The material's high optical limiting property is due to the RSA mechanism, which is the predominant NLO phenomenon [26]. Materials exhibiting RSA are characterized by their absorption cross sections in both the excited state and ground state. RSA produces an excited state with a greater magnitude than the ground state. The excited-state absorption cross-section ( $\sigma_{exc}$ ) and ground-state absorption cross-section ( $\sigma_{gr}$ ) of the natural dye are directly related to the dye's  $\beta$  value, which is calculated by [24].

$$\beta = \frac{\lambda N_o \Delta\sigma}{4\pi I_s} \quad (2)$$

where  $N_o$  is the number of molecules in a cubic unit,  $\lambda$  is the wavelength of laser source,  $I_s$  is the saturation intensity and  $\Delta\sigma = \sigma_{exc} - \sigma_{gr}$ . The ground-state absorption cross-section ( $\sigma_{gr}$ ) is given by [27],

$$\sigma_{gr} = \frac{\alpha_o}{N_o} \quad (3)$$

The estimated values of  $\sigma_{gr}$  and  $\sigma_{exc}$  of the natural dye derived from *chrysanthemum* petals is found to be the order of  $10^{-21} \text{ m}^2$  and  $10^{-17} \text{ m}^2$ , respectively. The value of  $\sigma_{exc}$  is four orders greater than  $\sigma_{gr}$  and conclude that RSA is the

predominant NLO mechanism observed in natural dye. According to the reference [24], the NLO coefficient of absorption transmittance in an OA profile can be determined by,

$$T(z, s = 1) = \sum_{m=0}^{\infty} \frac{[-q_0(z)]^m}{[m+1]^2}, \text{ for } |q_0(0)| < 1 \quad (4)$$

where

$$q_0 = \frac{\beta I_0 L_{eff}}{(1 + Z^2/Z_0^2)} \quad (5)$$

where  $L_{eff}$  is the sample effective length and  $Z_0$  is the diffraction length of the natural dye. The  $\beta$  of the natural dye derived from *chrysanthemum* petals is given by,

$$\beta = \frac{2\sqrt{2}\Delta T}{I_0 L_{eff}} \left(\frac{cm}{W}\right) \quad (6)$$

The CA Z-scan approach determines the magnitude and sign of the NLO refractive index for the natural dye which is depicted in Fig. 6. The transmittance curve of the natural dye exhibits self-defocusing nonlinearity, characterized by a pre-focal peak followed by a post-focal valley. Thermal nonlinearity occurs when a light source continuously absorbed by the sample and causes self-defocusing. Thermal lensing arises from a temperature change within the material caused by exposure to a CW laser. With an increase in temperature, the refractive index of the medium changes and the sample exhibits a negative index of refraction, causing it to behave as a defocusing lens. Self-defocusing of the extracted natural pigment occurs due to thermal effects, where the refractive index ( $n$ ) of the medium is defined as  $n = n_0 + n_2 I$ . In this equation,  $n_0$  represents the linear refractive index, and  $I$  stand for the intensity of the incident beam. The thermal lensing effect occurs due to laser-induced thermal changes, caused by the intermittent heat produced when a Gaussian laser beam is absorbed in the sample. This leads to variations in the refractive index within the laser gain medium, impacting the output laser power and beam quality. The thermally induced change in refractive index is known as "thermal lensing" and it is determined by a thermo-optic coefficient. The ability of the material to exhibit thermal lensing depends on the absorption of laser energy, resulting in the development of an inhomogeneous spatial nonlinear refractive index which behaves as a divergent lens, defocusing the laser beam and producing spatial variations in the output laser profile [28-29]. To calculate the thermo-optic coefficient ( $dn/dt$ ) of the natural pigment, the following equation is used:  $(dn/dt) = 4n_2 K / \alpha_0 \omega_0^2$ , where  $K$  is the thermal conductivity of water, and  $\alpha_0$  and  $\omega_0$  represent the linear absorption coefficient and beam waist at the focus, respectively. A large thermo-optic coefficient of the

natural dye is observed and calculated to be  $-3.67 \times 10^{-6} \text{ K}^{-1}$ .

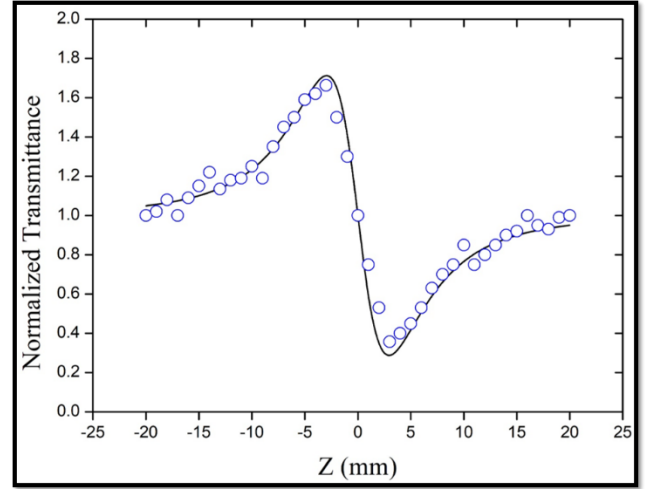


Fig. 6. CA Z-scan result of the natural dye derived from *chrysanthemum* petals (color online)

Furthermore, a third-order phenomenon becomes apparent when the distance between peak and valley is more significant than 1.7 times the Rayleigh length. The normalized transmittance of the natural dye is given by,

$$T(z) = 1 - \Delta\phi_0 \frac{4X}{(X^2 + 1)(X^2 + 9)} \quad (7)$$

where  $X = Z/Z_0$ .

The NLO index of refraction of the sample is determined by,

$$n_2 = \frac{\Delta\phi_0 \lambda}{2\pi I_0 L_{eff}} \left(\frac{cm^2}{W}\right) \quad (8)$$

where  $I_0$  is the beam intensity,  $\Delta\phi_0$  is the on-axis phase shift and  $\lambda$  is the wavelength. The estimated values of  $n_2$  of natural dye is presented in Table 1.

The real and imaginary features of the third-order NLO susceptibility of the natural dye are received from  $n_2$  and  $\beta$  which are given by [24],

$$Re[\chi^{(3)}](esu) = \frac{10^{-4} \epsilon_0 c^2 n_0^2}{\pi} n_2 \left(\frac{cm^2}{W}\right) \quad (9)$$

$$Im[\chi^{(3)}](esu) = \frac{10^{-2} \epsilon_0 c^2 n_0^2 \lambda}{4\pi^2} \beta \left(\frac{cm}{W}\right) \quad (10)$$

where  $c$  is the velocity of light and  $\epsilon_0$  is the vacuum permittivity. The third-order NLO susceptibility of the natural dye derived from is given by [24],

$$\chi^{(3)} = \sqrt{(Re(\chi^{(3)})^2 + (Im(\chi^{(3)}))^2} (esu) \quad (11)$$

The second-order polarizability of the natural dye is directly proportional to the third-order NLO susceptibility and the relation is given by [30],

$$\gamma = \frac{\chi^3}{L^4 N} (\text{esu}) \quad (12)$$

The variable N represents the molecular density measured in  $\text{cm}^3$ , whereas L represents the local field factor, which is determined by the formula  $L = (n^2 + 2)/3$ . Table 1 displays the third-order NLO susceptibility and second-order hyperpolarizability of the natural dye extracted from *chrysanthemum* petals. We notice a significant NLO susceptibility and compare our results with those of several natural dyes mentioned in Table 2. The NLO susceptibility of the natural dye obtained from *chrysanthemum* petals is higher than that of the natural dyes mentioned in the literature [31-40].

Table 1. Third-order NLO features of the natural dye derived from *chrysanthemum* petals

Parameters	Value
Wavelength of the light source	405 nm
Rayleigh length	3.28 mm
Nonlinear index of refraction ( $n_2$ )	$4.29 \times 10^{-7} \text{ cm}^2/\text{W}$
Nonlinear coefficient of absorption ( $\beta$ )	$2.01 \times 10^{-2} \text{ cm/W}$
Real part of the third-order NLO susceptibility ( $\text{Re}(\chi^3)$ )	$1.39 \times 10^{-6} \text{ esu}$
Imaginary part of the third-order NLO susceptibility ( $\text{Im}(\chi^3)$ )	$0.21 \times 10^{-6} \text{ esu}$
Third-order NLO susceptibility ( $\chi^3$ )	$1.41 \times 10^{-6} \text{ esu}$
Second-order hyperpolarizability ( $\gamma$ )	$1.02 \times 10^{-30} \text{ esu}$

Table 2. Third-order NLO features of the natural dyes derived from plant leaves, roots, fruits and flowers

Natural dye	wavelength	$n_2$ ( $\text{cm}^2/\text{W}$ )	$\beta$ ( $\text{cm/W}$ )	$\chi^3$ (esu)	References
Natural dye derived from <i>chrysanthemum</i> petals	405 nm	$-4.29 \times 10^{-7}$	$2.01 \times 10^{-2}$	$1.41 \times 10^{-6}$	Present work
Natural pigment derived from Aloe Vera plant	635 nm	$-2.31 \times 10^{-8}$	$2.42 \times 10^{-3}$	$7.93 \times 10^{-8}$	[31]
Chlorophyll-a extracted from <i>Andrographis paniculata</i> leaves	635 nm	$-4.29 \times 10^{-7}$	$-4.57 \times 10^{-3}$	$1.53 \times 10^{-6}$	[32]
Anthocyanin extracted from blueberry	635 nm	$-2.07 \times 10^{-7}$	$-2.19 \times 10^{-3}$	$5.28 \times 10^{-7}$	[33]
Lycopene extracted from tomato	650 nm	$-7.26 \times 10^{-8}$	$-0.20 \times 10^{-3}$	$2.65 \times 10^{-6}$	[34]
Chlorophyll extracted from <i>Coleus amboinicus</i>	650 nm	$-1.96 \times 10^{-7}$	$6.06 \times 10^{-3}$	$6.75 \times 10^{-7}$	[35]
Natural Pigment extracted from <i>Ocimum tenuiflorum</i>	650 nm	$-3.92 \times 10^{-7}$	$3.35 \times 10^{-2}$	$1.45 \times 10^{-6}$	[36]
Hibiscus Sabdariffa dye	515 nm	-	$-2.7 \times 10^{-11}$	-	[37]
Curcumin	473 nm	$6.86 \times 10^{-7}$	$2.23 \times 10^{-3}$	-	[38]
Olive oil blended turmeric	532 nm	$-8.52 \times 10^{-7}$	-	-	[39]
Betanin extracted from red beet root	532 nm	-	$1.59 \times 10^{-8}$	-	[40]

#### 4. Conclusion

The Z-scan approach was employed to investigate the third-order NLO characteristics of a naturally occurring dye derived from *chrysanthemum* petals. The UV-visible absorption spectrum revealed that the maximum absorption was observed in the visible region. FT-IR technique was utilized to determine the specific functional groups that are present in the natural dye. The  $n_2$  and  $\beta$  of the natural dye were found to be of the order of  $10^{-7} \text{ cm}^2/\text{W}$  and  $10^{-2} \text{ cm/W}$ , respectively. The NLO index of refraction was due to thermal nonlinearity, while the NLO absorption coefficient was attributed to RSA. The origin of self-defocusing effect was due to thermal nonlinearity and the thermo-optic coefficient of the natural dye was observed to be  $-3.67 \times 10^{-6} \text{ K}^{-1}$ .

The natural dye's third-order NLO susceptibility and second-order hyperpolarizability were determined to be about  $10^{-6} \text{ esu}$  and  $10^{-30} \text{ esu}$ , respectively. The findings indicate that the organic pigment derived from *chrysanthemum* petals has potential utility in optical limiting and switching applications.

#### Acknowledgments

The authors express their sincere appreciation to the Researchers Supporting Project Number (RSP2025R143) King Saud University, Riyadh, Saudi Arabia.

## References

- [1] M. C. Sreenath, I. Hubert Joe, V. K. Rastogi, *Optics and Laser Technology* **108**, 218 (2018).
- [2] G. Vinitha, A. Ramalingam, *Laser Physics* **18**, 1176 (2008).
- [3] K. Jamshidi-Ghaleh, S. Salmani, M. H. Majles Ara, *Optics Communications* **271**, 551 (2007).
- [4] V. G. Sreeja, G. Vinitha, R. Reshmi, E. I. Anila, M. K. Jayaraj, *Optical Materials* **66**, 460 (2017).
- [5] N. Priyadarshani, T. C. Sabari Girisun, S. Venugopal Rao, *Optical Materials* **88**, 586 (2019).
- [6] H. Motiei, A. Jafari, R. Naderali, *Optics and Laser Technology* **88**, 68 (2017).
- [7] Q. M. A. Hassan, P. K. Palanisamy, *Modern Physics Letters B* **20**, 623 (2006).
- [8] P. Gheorghe, A. Petris, A. M. Anton, *Polymers* **16**(1), 96 (2024).
- [9] A. Petris, I. C. Vasiliu, P. Gheorghe, A. M. Iordache, L. Ionel, L. Rusen, S. Iordache, M. Elisa, R. Trusca, D. Ulieru, S. Etemadi, R. Wendelbo, J. Yang, K. Thorshaug, *Nanomaterials* **10**, 1638 (2020).
- [10] Jancy John, Vinoy Thomas, Ramakrishnan Jayakirshnan, Ibrahimkutty Rejeena, Sebastian Mathew, Abdulhassan Mujeeb, Roseleena Thomas, *J. Optoelectron Adv. M.* **25**(1-2), 12 (2023).
- [11] Mohd Mehkoom, Abid Ali, Mohammad Jane Alam, Farman Ali, S. M. Afzal, Shabbir Ahmad, *Journal of Molecular Structure* **1278**, 134921 (2023).
- [12] Abdu Saeed, Mir. A N Razvi, Numan Salah, *Results in Physics* **24**, 104162 (2021).
- [13] S Deepa, S. Madhu, S. Devasenan, G. Murali, P. D. Pancharatna, M. Maaza, K. Kaviyarasu, S. Jeyaram, *Journal of Fluorescence* **34**, 1885 (2023).
- [14] K. Bouchouit, Beata Derkowska-Zielinska, Anna Migalska-Zalas, S. Abed, N. Benali-Cherif, B. Sahraoui, *Dyes and Pigments* **86**, 161 (2010).
- [15] Brahim Kouissa, K. Bouchouit, S. Abed, Z. Essaidi, B. Derkowska, B. Sahraoui, *Optics Communications* **293**, 75 (2013).
- [16] S. Zongo, K. Sanusi, J. Britton, P. Mthunzi, T. Nyokong, M. Maaza, B. Sahraoui, *Optical Materials* **46**, 270 (2015).
- [17] A. P. Veduta, B. P. Kirsanoy, *Journal of Experimental and Theoretical Physics* **27**(5), 736 (1968).
- [18] B. Buchalter, G. R. Meredith, *Applied Optics* **21**, 3221 (1982).
- [19] R. Adair, L. L. Chase, S. A. Payne, *Journal of the Optical Society of America B* **4**(6), 875 (1987).
- [20] A. Petris, P. Gheorghe, T. Braniste, I. Tiginyanu, *Materials* **14**, 3194 (2021).
- [21] A. Petris, P. S. Gheorghe, V. I. Vlad, E. Rusu, V. V. Ursaki, I. M. Tiginyanu, *Optics Materials* **76**, 69 (2018).
- [22] A. Petris, Pe. Gheorghe, I. Rau, A.-M. Manea-Saghin, F. Kajzar, *European Polymer Journal* **110**, 130 (2019).
- [23] A. Petris, P. Gheorghe, V. I. Vlad, I. Rau, F. Kajzar, *Romanian Reports in Physics* **67**, 1373 (2015).
- [24] M. Sheik- Bahae, A. A. Said, T. Wei, D. J. Hagan, E. W. Van Stryland, *IEEE Journal of Quantum Electronics* **26**, 760 (1990).
- [25] S. Jeyaram, *Journal of Fluorescence* **34**, 313 (2024).
- [26] N. Priyadarshani, T. C. Sabari Girisun, S. Venugopal Rao, *Optics Materials* **88**, 586 (2019).
- [27] M. D. Zidan, A. Arfan, A. Allahham, *Spectrochimica Acta Part A* **190**, 135 (2018).
- [28] M. D. Zidan, A. W. Allaf, A. Allahham, A. Alzier, *Optik* **200**, 163175 (2020).
- [29] S. Arun Kumar, J. Senthilselvan, G. Vinitha, *Optics and Laser Technology* **109**, 561 (2019).
- [30] Hussain A. Badran, Hanan A Al-Hazam, R. K. Fakher Alfahed, Khalid I. Ajeel, *Journal of Materials Science: Materials in Electronics* **32**, 14623 (2021).
- [31] S. Jeyaram, *Brazilian Journal of Physics* **52**, 24 (2022).
- [32] S. Jeyaram, T. Geethakrishnan, *Optics and Laser Technology* **116**, 31 (2019).
- [33] S. Jeyaram, T. Geethakrishnan, *Results in Physics* **1**, 100010 (2020).
- [34] N. Numan, S. Jeyaram, K. Kaviyarasu, P. Neethling, J. Sackey, C. L. Kotsedi, M. Akbari, R. Morad, P. Mthunzi-Kufa, B. Sahraoui, M. Maaza *Scientific Reports* **12**, 9078 (2022).
- [35] B Anusha, Sandhanasamy Devanesan, Mohamad S. Al. Salhi, G. Murali, M. Vimalan, S. Madhu, S. Jeyaram, *Journal of Optics* **2024**, s12596 (2024).
- [36] S. Jeyaram, D. Jeancy Rany, *Journal of Fluorescence* **33**, 287 (2023).
- [37] Aya Abu Baker, Ganjaboy S. Boltaev, Piotr Piatkowski, Mustafa Khamis, Ali S. Alnaser, *Optical Materials* **138**, 113728 (2023).
- [38] Ayman G. Faisal, Qusay M. A. Hassan, Tahseen A. Alsalmim, H. A. Sultan, Fadhil Kamounah, C. A. Emsary, Kawkab Ali Hussein, Ali Hussein *Optik* **306**, 171800 (2024).
- [39] Z. Mousavi, B. Ghafary, M. H. Majles Ara, *Journal of Molecular Liquids* **285**, 444 (2019).
- [40] Aparna Thankappan, Sheenu Thomas, V. P. N. Nampoore, *Optical Materials* **35**, 2332 (2013).

\*Corresponding author: jeyaram.msc@gmail.com